

Quantum Fuel with Multilevel Atomic Coherence for Ultrahigh Specific Work in a Photonic Carnot Engine

Deniz Türkpençe¹ and Özgür E. Müstecaplıoğlu^{1,*}

¹*Department of Physics, Koç University, İstanbul, Sarıyer 34450, Turkey*

(Dated: June 9, 2019)

We investigate scaling of work output and efficiency of a photonic Carnot engine with the number of quantum coherent resources. Specifically, we consider a generalization of the “phaseonium fuel” for the photonic Carnot engine, which was first introduced as a three-level atom with two lower states in a quantum coherent superposition by [M. O. Scully, M. Suhail Zubairy, G. S. Agarwal, and H. Walther, *Science* **299**, 862 (2003)], to the case of $N + 1$ level atoms with N coherent lower levels. Deriving a multilevel mesoscopic master equation for the system, we evaluate the harvested work by the engine, and its efficiency. We find that efficiency and extracted work scale quadratically with the number of quantum coherent levels. Quantum coherence boost to the specific energy (work output per unit mass of the resource) is a profound fundamental difference of quantum fuel from classical resources. Besides, we examine the dependence of cavity loss on the number of atomic levels and find that multilevel phaseonium fuel can be utilized to beat the decoherence due to cavity loss. Our results bring the photonic Carnot engines much closer to the capabilities of current resonator technologies.

PACS numbers: 42.50.Ar,05.70.-a,07.20.Pe

A practical figure of merit to compare fuel and battery materials is the specific energy, or energy to mass ratio [1–3]. As a material constant, it measures the energy that will be harvested by using a unit mass of the material. About a decade ago, a highly non-traditional fuel, called “phaseonium”, which is a three level atom with two lower states in a quantum coherent superposition, was proposed to be used in a photonic Carnot engine [4]. Phaseonium engine could work with a single heat bath and could operate beyond Carnot efficiency [4–7]. This proposal stimulated much interest to quantum heat engines [8–16]. It was later argued that existing resonator systems can not implement such an engine, due to high cavity losses and atomic dephasing [17]. In this letter, we address a fundamental question of how the specific energy of phaseonium fuel is scaled with the number of quantum coherent levels. A favorable scaling law against decoherence and dephasing could bring the phaseonium engine closer to available practical systems.

We describe multilevel generalization of phaseonium fuel in Fig. 1. The block diagonal density matrix ρ of an $N + 1$ level atom is shown in Fig. 1a. The excited level, denoted by “ a ”, and the lower levels, denoted by “ b_1, b_2, \dots, b_N ” are well separated from each other by an energy Ω measured from the central lower level $b_{N/2}$ as shown in Fig. 1b. The lower levels can be degenerate or non-degenerate. The diagonal elements ρ_{aa} , and ρ_{bb} , with $b \in \{b_1, b_2, \dots, b_N\}$, determine the level populations, while the off diagonal elements $\rho_{bb'}$, with $b' \neq b$, indicate the coherence between the levels. Coherence can be characterized by the magnitude and phase of the complex number $\rho_{bb'}$. Though both the amplitude and the phase of coherent superposition states can be controlled in experiments [18], the main control variable for the pho-

tonic Carnot engine is the phase of the coherence as the amplitude is required to be small enough to keep the system only slightly out of thermal equilibrium. The complete graphs in Fig. 1a have N nodes and $N(N - 1)/2$ links, representing the atomic energy levels and the coherences between them, respectively. The simplest graph has $N = 2$ nodes, which is the case of the original phaseonium proposal [4]. The interplay between quantum coherence and energy discussed in photon Carnot engine [4] revealed that the energy content of the phaseonium with $N = 2$ can be optimized at a certain phase of the coherence. We could envision as if we are considering more complex, larger, phaseonium molecules with the graphs having $N > 2$, corresponding to $N + 1$ level atom phaseonium (NLAP).

We can imagine different phaseonium molecules can be possible for a given atom of unit mass and explore how the specific energy of the atom depends on the size of the phaseonium molecule characterized by N . Next to the phase of coherence, N becomes another control parameter which could favorably contribute to the enhancement of the specific energy of the single atom quantum fuel. For $N \gg 1$, the number of coherences would scale quadratically, $\sim N^2$. If the quadratic coherence scaling could be translated into the energy content of the atomic fuel, we could overcome the cavity losses for implementation and boost the performance of quantum Carnot engine for applications. From fundamental point of view, such scaling analysis could reveal profound difference of quantum fuel from a classical resource as such a scaling cannot exist without quantum coherence.

The operation of photonic Carnot engine is described in Fig. 2. The working fluid of the engine is the photon gas in a high quality single mode cavity of frequency Ω .

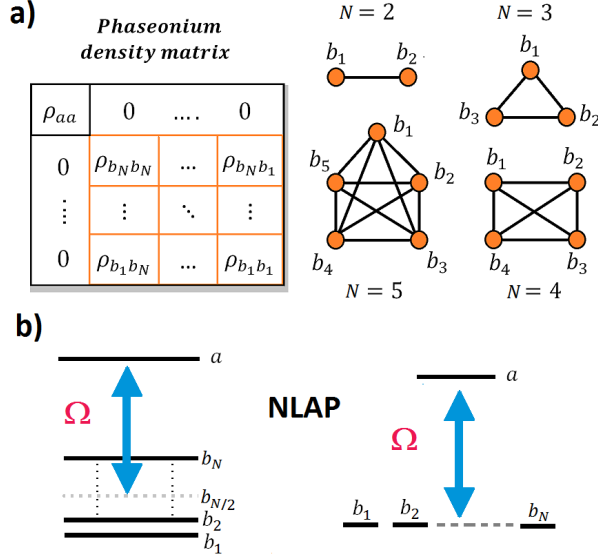


Figure 1. (Color online) $N+1$ level atom phaseonium (NLAP) fuel. a) Density matrix ρ and complete graph representations of NLAP. ρ is $N+1$ dimensional square matrix. Its coherent block can be represented by a complete graph with N nodes and $S = N(N-1)/2$ links. Graphs were shown up to $N=5$ number of nodes. b) NLAP for non-degenerate and degenerate atoms. The excited state is denoted by a and the lower levels are denoted by b_i with $i = 1..N$. The upper level is well separated from the lower levels by an energy $\hbar\Omega$ measured from the central lower level $b_{N/2}$.

The radiation pressure by the cavity photons applies on the cavity mirrors playing the role of the piston of the engine. The quantum fuel of the engine is an NLAP. The quantum Carnot cycle consists of two quantum isothermal and two quantum adiabatic processes.

In the isothermal expansion, NLAPs are generated and injected into the cavity at a rate r . The interaction time τ between an NLAP and the cavity field is short, $\tau < 1/r$, so that only one NLAP can be present in the cavity [19]. Coherences in NLAP are characterized by $N(N-1)/2$ phase parameters ϕ_{ij} , with $i, j = 1, 2, \dots, N$. Coherent superposition states in $N+1$ level atom system can be generated by stimulated Raman adiabatic passage [20, 21], Morris-Shore transformation [22], or quantum Householder reflection techniques [23]. Thermalization of the single atom can be considered relatively fast and hence the injection rate would be limited by the time of coherence preparation. The choice of specific technique of coherence induction depends on the details of a particular implementation. If the amplitudes of the coherences are much smaller than the level populations, then NLAP can be assumed in an approximate thermal equilibrium with a thermal reservoir (hohlraum) at a temperature T_h . During the interaction, the mean number of photons, \bar{n} , and the cavity temperature increases; while the

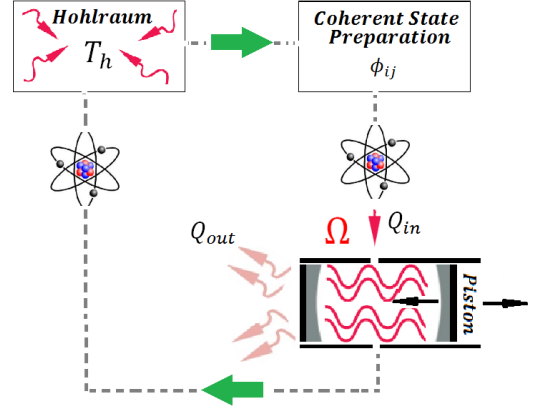


Figure 2. (Color online) Photonic Carnot engine with $N+1$ level atom phaseonium (NLAP) fuel. Photon gas in a high quality cavity of frequency Ω is the working substance and the mirrors of the cavity play the role of the piston. NLAP leaves the hohlraum at temperature T_h and is induced quantum coherence among its lower levels characterized by $N(N-1)/2$ phase parameters ϕ_{ij} with $i, j = 1..N$. Created NLAPs are repeatedly injected into the cavity at a rate r in the quantum isothermal expansion process, where heat Q_{in} is transferred to the cavity. The cycle continues with quantum adiabatic expansion and quantum isothermal compression and is completed with a quantum adiabatic compression. An amount of heat Q_{out} is rejected into the entropy sink in the isothermal compression.

expansion cools down the empty cavity. Repeated injection of NLAPs into the cavity maintains the cavity field at a temperature T_ϕ by transferring a total amount of heat into the cavity as Q_{in} . T_ϕ is an effective temperature defined in terms of the steady state photon number \bar{n}_ϕ as $T_\phi = \hbar\Omega/k \ln(1 + 1/\bar{n}_\phi)$, with k is the Boltzmann constant. It can be higher than T_h in the presence of coherence [4]. The cavity volume, and hence the frequency, change negligibly, $\Delta\Omega \ll \Omega$.

The cycle continues with an adiabatic expansion where the entropy remains constant and the temperature drops as the Ω changes appreciably. Following step is the isothermal compression in which heat Q_{out} is transferred from cavity to a cold reservoir at a temperature T_c . The cycle is completed by adiabatic compression where the temperature is raised back to T_ϕ .

The net work extracted from the cycle is $W_{net} = Q_{in} - Q_{out}$ where $Q_{in} = T_\phi(S_2 - S_1)$ and $Q_{out} = T_c(S_3 - S_4)$. The mean photon number \bar{n}_i and the temperature T_i at the beginning of the i^{th} stage determine the entropy S_i by $S_i = k \ln(\bar{n}_i + 1) + \hbar\Omega\bar{n}_i/T_i$. Using $S_1 = S_4$, $S_2 = S_3$, $T_1 = T_2 = T_\phi$, and $T_3 = T_4 = T_c$, we write $W_{net} = (T_\phi - T_c)(S_2 - S_1)$. The efficiency of the engine is defined as $\eta = W_{net}/Q_{in}$. It reduces to $\eta = 1 - T_h/T_\phi$. This is the standard definition of thermodynamic efficiency in Carnot cycle; though the overall efficiency of the engine

should include the cost of the preparation of the quantum coherent atom; which would ensure the validity of the second law [7]. During the adiabatic process \bar{n} does not change so that $\bar{n}_1 = \bar{n}_4 = (\exp(\hbar\Omega/kT_c) - 1)^{-1}$ and $\bar{n}_2 = \bar{n}_\phi$. These relations reveal that work and efficiency of the photonic Carnot engine can be calculated by determining the \bar{n}_ϕ at the end of the isothermal expansion stage.

In order to find the \bar{n}_ϕ , we solve $\dot{\bar{n}}_\phi = \sum_n n \dot{\rho}_{nn} = 0$ where $\dot{\rho}_{nn} = \langle n | \dot{\rho} | n \rangle$. Here $|n\rangle$ is the Fock number state for the cavity photons and ρ is the reduced density matrix of the cavity field. The equation of motion for ρ can be obtained by tracing the equation of motion of the complete system over atomic degrees of freedom

$$\dot{\rho}_{nn} = -\frac{i}{\hbar} \sum_k (Tr_{at}[H^k, \rho^k]_{nn}), \quad (1)$$

where $H^k = H_0 + H_I^k$ is the Hamiltonian of the arbitrary k^{th} atom in the interaction picture relative to the cavity photons, with $H_0 = \hbar\omega_a|a\rangle\langle a| + \hbar\sum_{i=1}^N \omega_{b_i}|b_i\rangle\langle b_i|$ and $H_I^k = \hbar g \sum_{i=1}^N |a\rangle\langle b_i| \hat{a} e^{-i\Omega t} + H.c..$ Here $\hbar\omega_a$, $\hbar\omega_{b_i}$ are the energies of atomic states $|a\rangle$ and $|b_i\rangle$, with $i = 1..N$, g is the coupling rate between the atom and the field, and \hat{a} is the photon annihilation operator. The model Hamiltonian describes a situation where $N + 1$ level atom is coupled to a single mode cavity in a fan shaped transition scheme. A more realistic model requires consideration of multimode cavity coupled to an atom with multiple upper and lower hyperfine levels [24, 25]. Such models can be reduced to effective single mode cavity and multilevel atom interactions [24] or can be directly described by generalized master equations of micromasers [26]. Atoms with fan shaped degenerate level schemes are also studied from the perspective of generating large superposition states [20, 27]. The central question for us here is the dependence of work and efficiency on the number of the superposed quantum states and we will only consider single upper level and a set of degenerate or non-degenerate lower levels for simplicity.

Analytically calculating the right hand side of the Eq. (1), we find (see Supplement [28])

$$\begin{aligned} \dot{\rho}_{nn} = & -rg^2 \{ K_a \rho_{aa} [(n+1)\rho_{nn} - n\rho_{n-1, n-1}] \\ & + \left(\sum_{i=1}^N K_{b_i} \rho_{b_i b_i} + \sum_{i < j} K_{ij}^{\phi_{ij}} |\rho_{b_i b_j}| \right) \\ & \times [n\rho_{nn} - (n+1)\rho_{n+1, n+1}] \}, \end{aligned} \quad (2)$$

where $K_a = 2 \sum_{i=1}^N 1/(\Delta_i^2 + \gamma^2)$, $K_{b_i} = 2/(\Delta_i^2 + \gamma^2)$ and $K_{ij}^{\phi_{ij}} = [2 \cos \phi_{ij} (\Delta_i \omega_{b_i b_j} + \gamma^2) + 2\gamma \sin \phi_{ij} (\omega_{b_i b_j} - \Delta_i)] / (\Delta_i^2 + \gamma^2)(\omega_{b_i b_j}^2 + \gamma^2) + [2 \cos \phi_{ij} (\gamma^2 - \Delta_j \omega_{b_i b_j}) + 2\gamma \sin \phi_{ij} (\omega_{b_i b_j} + \Delta_j)] / (\Delta_j^2 + \gamma^2)(\omega_{b_i b_j}^2 + \gamma^2)$. Here γ is the atomic decay constant, $\Delta_i = \omega_{ab_i} - \Omega$, $\omega_{ab_i} = \omega_a - \omega_{b_i}$, $\omega_{b_i b_j} = \omega_j - \omega_i$. Thus we obtain the rate of change of average photon number [28]

$$\dot{\bar{n}}_\phi = rg^2 \{ K_a \rho_{aa} (\bar{n}_\phi + 1) - (R_{g_0} + R_{g_c}) \bar{n}_\phi \}, \quad (3)$$

where $R_{g_0} = \sum_{i=1}^N K_{b_i} \rho_{b_i b_i}$ and $R_{g_c} = \sum_{i < j} K_{ij}^{\phi_{ij}} |\rho_{b_i b_j}|$. Solving Eq. (3) in the steady state, we obtain

$$\bar{n}_\phi = \frac{\bar{n}}{1 + \bar{n} \frac{R_{g_c}}{K_a \rho_{aa}}}, \quad (4)$$

where $\bar{n} = (R_{g_0}/K_a \rho_{aa} - 1)^{-1}$ is the average photon number in the absence of coherence. Using $\bar{n}_\phi = (\exp(\hbar\Omega/kT_\phi) - 1)^{-1}$, we determine the effective cavity temperature as

$$T_\phi = \frac{T_h}{1 + \bar{n} \frac{R_{g_c}}{K_a \rho_{aa}}}, \quad (5)$$

by using high temperature approximations $\bar{n}_\phi \approx kT_\phi/\hbar\Omega$ and $\bar{n} \approx kT_h/\hbar\Omega$ in Eq. (4).

Therefore, the efficiency of the photonic Carnot engine in the case of NLAP becomes

$$\eta_\phi = \eta_c - \frac{T_c}{T_h} \bar{n} \frac{R_{g_c}}{K_a \rho_{aa}}, \quad (6)$$

where $\eta_c = 1 - T_c/T_h$ is the Carnot efficiency. Note that for $T_c = T_h$, $\eta_c = 0$ but η_ϕ could have a positive value for particular values of control parameters $\phi_1, \phi_2, \dots, \phi_S$. In order to get further analytical results we will make some simplifying assumptions.

We focus on degenerate NLAP case to proceed analytically, for which $E_a = \Omega$, $E_{b_i} = 0, i = 1..N$, $\omega_{ab_i} = \Omega$, $\Delta_i = 0$, $\omega_{b_i b_j} = 0$ and $K_a = 2N/\gamma^2$. In addition, we consider phase locked equal amplitude coherences with $\phi_{ij} = \phi$ and $|\rho_{b_i b_j}| = \lambda$. Hence the coefficients in Eq. (2) become $K_{ij}^{\phi_{ij}} = 4 \cos \phi / \gamma^2$, $R_{g_0} = 2NP_g/\gamma^2$ and $R_{g_c} = 2N(N-1) \cos \phi \lambda / \gamma^2$, and hence Eq. (3) reduces to

$$\dot{\bar{n}}_\phi = 2\mu N [(P_e - P_g + N\xi\lambda)\bar{n}_\phi + P_e] - \kappa \bar{n}_\phi, \quad (7)$$

for $N \gg 1$, $\phi = \pi$, where $\mu = rg^2/\gamma^2$, $P_e = \rho_{aa} = \exp(-\beta E_a)/Z$, $P_g = \rho_{b_i b_i} = 1/Z$ with $Z = \exp(-\beta E_a) + N$. Here we introduced κ and ξ , with $|\xi| < 1$, as the decoherence rate due to the dissipation in the cavity and a phenomenological decoherence factor due to atomic dephasing, respectively [17].

Steady state solution of the Eq. (7) yields an effective temperature given by $T_\phi = T_h/(1 + F(T_h))$ in the high temperature limit where

$$F(T_h) = \frac{\bar{n}}{P_e} \left(-N\xi\lambda + \frac{\kappa}{2N\mu} \right), \quad (8)$$

with $\bar{n} = P_e/(P_g - P_e)$. For small coherence and decoherence terms in $F(T_h)$, an approximate expression can be written for the effective temperature

$$T_\phi = T_h \left(1 + N^2 \xi \lambda \bar{n} - \frac{\kappa}{2\mu} \bar{n} \right). \quad (9)$$

This result shows that if the reduction of the magnitude of coherence due to dephasing is slower than the

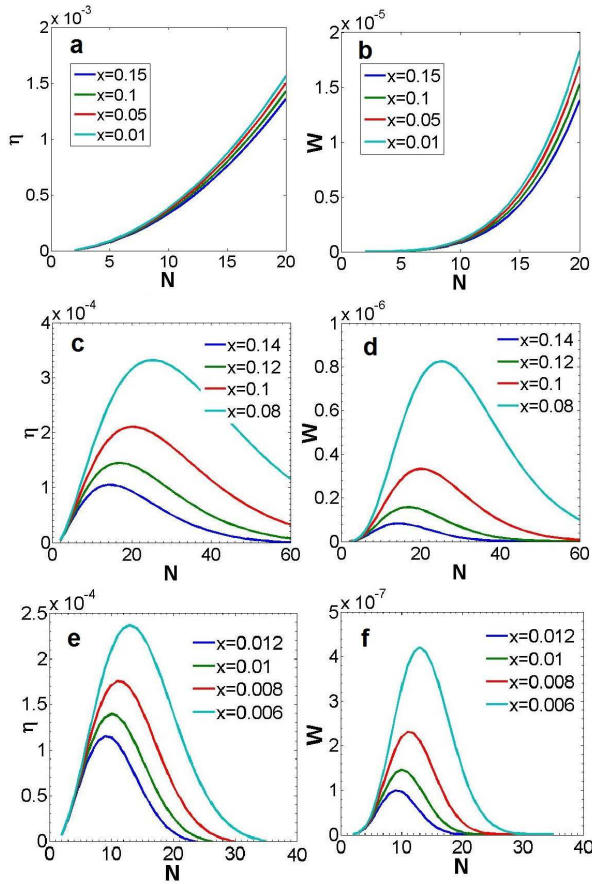


Figure 3. (Color online) Extracted work (W) and efficiency (η) of photonic Carnot engine, with $N + 1$ level atom phaseonium (NLAP) fuel, depending on the number of degenerate coherent ground state levels N , for different decoherence factor models (a)-(b) $\xi = \exp(-x)$, (c)-(d) $\xi = \exp(-Nx)$. (e)-(f) $\xi = \exp(-N^2x)$, where $x = t_{\text{int}}/T_2$ is the ratio between t_{int} atom-field interaction time and the T_2 atomic dephasing time. The plots are given for the circuit QED parameters in Ref. [17]. The quantities $g = 0.01$, $r = 1 \times 10^{-4}$, $\kappa = 6.25 \times 10^{-4}$, and $\gamma = 5 \times 10^{-6}$, which are the coupling coefficient to the cavity field, atomic injection rate, cavity loss term, and atomic decay respectively, are dimensionless and scaled with the resonance frequency $\Omega \sim 10$ GHz.

quadratic increase with N , then the multilevel coherence could be used to beat the decoherence by the cavity dissipation.

In the high temperature limit ($T \gg \Omega$), the entropy change in the isothermal expansion stage is $\Delta S = k\Delta\Omega/\Omega$ and the heat input becomes $Q_{\text{in}} = T_h\Delta S$. The work output at $T_h = T_c$ is found to be $W = Q_{\text{in}}\eta$ where $\eta = \bar{n}(N^2\xi\lambda - \kappa/2\mu)$, respectively. In superconducting circuit, microwave and optical resonators, it is estimated that $\kappa/2\mu\xi\lambda \sim 10$ [17]. N^2 should be replaced by $N(N-1)/2$ for smaller number of levels. Accordingly, by using five or more level quantum phaseonium fuel, the

working fluid can beat quantum decoherence to harvest positive work. In Fig. 3, we plot the work output and efficiency of the photonic Carnot engine with degenerate NLAP fuel, depending on the number of quantum coherent levels. We consider N independent as well as N dependent scaling models for the decoherence factor and take $\xi = \exp(-x)$ in Fig. 3(a)-(b), $\xi = \exp(-Nx)$ in Fig. 3(c)-(d), and $\xi = \exp(-N^2x)$ in Fig. 3(e)-(f), where $x = t_{\text{int}}/T_2$ is the ratio between t_{int} atom-field interaction time and the T_2 atomic dephasing time. The plots are given for the circuit QED parameters in Ref. [17]. We consider larger atomic dephasing rates than the typical values to demonstrate its limiting effect on W and η . The plots indicate that even when there is large dephasing, which can increase with N linearly or quadratically, W and η can retain their quadratic power law with N up to a critical N . Similar results are found for the cases of optical and microwave cavities [28].

Summarizing, we examined scaling of work and efficiency of a quantum heat engine with the number of quantum resources. Specifically, we considered a photonic Carnot engine with a multilevel phaseonium quantum fuel. We derived a generalized master equation for the cavity photons, which forms the working fluid of the engine, and determined the steady state photon number to calculate the work output and thermodynamic efficiency. We find that they scale quadratically with the number of quantum coherent levels N . We examined the case of degenerate levels to get analytical results and to examine scaling laws against decoherence due to cavity dissipation and atomic dephasing. Using typical parameters in modern resonator systems, such as circuit QED, our calculations reveal that decoherence due to cavity dissipation could be overcome by the multilevel quantum coherence even in the presence of large dephasing rate. If the dephasing rate increases with N , then work and efficiency can still overcome the decoherence and retain their N^2 scaling up to a critical number of coherent levels.

Authors warmly thank N. Allen, A. Imamoglu and I. Adagideli for illuminating discussions. Authors acknowledge support from Koç University and Lockheed Martin University Research Agreement.

* omustecap@ku.edu.tr

- [1] S. G. Chalk and J. F. Miller, *J. of Power Sources* **159**, 73 (2006).
- [2] K. T. Chau, Y. S. Wong, and C. C. Chan, *Energy Convers. Manage.* **40**, 1021 (1999).
- [3] Y. Yang, M. T. McDowell, A. Jackson, J. J. Cha, S. S. Hong, and Y. Cui, *Nano Lett.* **10**, 1486 (2010).
- [4] M. O. Scully, M. S. Zubairy, G. S. Agarwal, and H. Walther, *Science* **299**, 862 (2003).
- [5] M. O. Scully, *AIP Conf. Proc.* **643**, 83 (2002).
- [6] Y. V. Rostovtsev, Z. E. Sariyanni, and M. O. Scully,

- Laser Phys. **13**, 375 (2003).
- [7] M. S. Zubairy, in *AIP Conference Proceedings*, Vol. 643 (AIP Publishing, 2002) pp. 92–97.
- [8] T. D. Kieu, Phys. Rev. Lett. **93**, 140403 (2004).
- [9] H. T. Quan, Y.-x. Liu, C. P. Sun, and F. Nori, Phys. Rev. E **76**, 031105 (2007).
- [10] A. E. Allahverdyan, R. S. Johal, and G. Mahler, Phys. Rev. E **77**, 041118 (2008).
- [11] R. S. Johal, Phys. Rev. E **80**, 041119 (2009).
- [12] J. Wang, J. He, and Z. Wu, Phys. Rev. E **85**, 031145 (2012).
- [13] M. O. Scully, K. R. Chapin, K. E. Dorfman, M. B. Kim, and A. Svidzinsky, PNAS **108**, 15097 (2011).
- [14] H. Li, J. Zou, W.-L. Yu, L. Li, B.-M. Xu, and B. Shao, EPJ D **67** (2013).
- [15] Z. Zhuang and S.-D. Liang, Phys. Rev. E **90**, 052117 (2014).
- [16] F. Altintas, A. Ü. C. Hardal, and Ö. E. Müstecaplıoğlu, Phys. Rev. E **90**, 032102 (2014).
- [17] H. T. Quan, P. Zhang, and C. P. Sun, Phys. Rev. E **73**, 036122 (2006).
- [18] F. Vewinger, M. Heinz, U. Schneider, C. Barthel, and K. Bergmann, Phys. Rev. A **75**, 043407 (2007).
- [19] P. Filipowicz, J. Javanainen, and P. Meystre, Phys. Rev. A **34**, 3077 (1986).
- [20] M. Amniat-Talab, M. Saadati-Niari, S. Guérin, and R. Nader-Ali, Phys. Rev. A **83**, 013817 (2011).
- [21] G. Bevilacqua, G. Schaller, T. Brandes, and F. Renzoni, Phys. Rev. A **88**, 013404 (2013).
- [22] M. Saadati-Niari and M. Amniat-Talab, J. Mod. Opt. **61**, 1492 (2014),.
- [23] P. A. Ivanov, B. T. Torosov, and N. V. Vitanov, Phys. Rev. A **75**, 012323 (2007).
- [24] K. M. Birnbaum, A. Boca, R. Miller, A. D. Boozer, T. E. Northup, and H. J. Kimble, Nature **436**, 87 (2005),.
- [25] K. J. Arnold, M. P. Baden, and M. D. Barrett, Phys. Rev. A **84**, 033843 (2011).
- [26] V. A. Reshetov and I. V. Yevseyev, Laser Phys. Lett. **1**, 124 (2004),.
- [27] E. S. Kyoseva and N. V. Vitanov, Phys. Rev. A **73**, 023420 (2006).
- [28] See Supplementary Material for more details.